[Article ID] 1003- 6326(2002)02- 0189- 04

Effects of Mo substituted Nb on magnetic properties of Finemet alloy①

LIANG Gong-ying(梁工英)[1], HUANG Yi-kun(黄一坤)[2], G. Friedman[2]
(1. Department of Materials Physics, Science School, Xi'an Jiaotong University, Xi'an 710049, China;
2. Department of Electrical Engineering and Computer Science, University of Illinois, Chicago, IL 60607, USA)

[Abstract] Different Mo contents have been added into traditional Finemet alloy to form $Fe_{73.5}Cu_1Nb_{3-x}Mo_xSi_{13}B_{9.5}$ (x= 0~ 3) alloys. The change in DC and AC magnetic properties with Mo for Nb substitution was investigated. The results show that, with adding Mo, although the DC relative permeability decreases and the coercive force increases slightly, the saturation flux density B_S can be increased, and the core loss of the alloy can be decreased. The AC permeability of samples contained Mo is higher than that of alloy without Mo content. $Fe_{73.5}Cu_1Nb_1Mo_2Si_{13}B_{9.5}$ alloy has the highest saturation flux density B_S. $Fe_{73.5}Cu_1Nb_2Mo_1Si_{13}B_{9.5}$ alloy has the best frequency dependence on the AC permeability and core loss.

[Key words] magnetic materials; nanocrystalline; soft magnetic properties
[CLC number] TM 274 [Document code] A

1 INTRODUCTION

Finemet alloys have been extensively studied since 1988[1~6]. A typical example of this material has the composition $Fe_{73.5}Cu_1Nb_3Si_{13}B_{9.5}$ (mole fraction, %)[7,8]. The materials are typically cast as amorphous ribbons. The subsequent heat treatment above crystallization temperature produces a homogeneous nanocrystalline structure of α-FeSi with a typical grain size of 10~ 20 nm[9,10]. The formation of the ultrafine grain structure is attributed to the addition of Cu and Nb[1]. Though similar effect of Nb and Mo addition to FeCuSiB alloys has been mentioned before[2], no report has been heard for the effect of magnetic properties on adding Nb and Mo elements together yet. Since Mo is cheaper and more accessible in nature than Nb, and since Mo may increase saturation flux density B_S and reduce core loss[11,12], it is very important to study Mo substitution. Such study is the focus of the present work.

2 EXPERIMENTAL

The $Fe_{73.5}Cu_1Nb_{3-x}Mo_xSi_{13}B_{9.5}$ (x= 0~ 3) alloys with partial substitution of Nb by Mo have been prepared by the single roller melt spinning method. The sample was wound into a core using amorphous ribbon. The core is 19 mm in outer diameter and 15 mm in inner diameter. Before measuring magnetic properties, the samples were heat annealed in argon protection for 1 h at various temperatures between 450 ℃ and 650 ℃. X-ray diffraction measurements were carried out using Cu K_α radiation. Crystallization temperatures of amorphous alloys were measured by a differential scanning calorimeter (DSC) at a heating rate of 10 K/min. The microstructures of annealed samples and crystallization behaviors of the amorphous alloys were also examined by JEM-200CX transmission electron microscope (TEM). TEM sample was prepared by electropolishing using a twin jet polisher. The change in magnetic properties with Mo content and annealing temperature was investigated. DC magnetic properties, such as, relative permeability μ_m, saturation flux density B_S and coercivity H_C, core loss P_C, were measured on the hysteresis loop by a DC measuring device of the impulsion method. AC magnetic properties, core loss P_C was measured using an electric bridge and AC relative permeability $|\tilde{\mu}|$ was measured on a B-H loop tracer. The measured frequency range of AC magnetic properties was from 50 Hz to 10 kHz.

3 RESULTS AND DISCUSSION

3.1 Effect of content of Mo on optimum annealing temperature

Fig. 1 shows the change in beginning, peak and end crystallization temperatures of $Fe_{73.5}Cu_1Nb_{3-x}Mo_xSi_{13}B_{9.5}$ (x= 0~ 3) amorphous alloys as the content of Nb and Mo changes. When the content of Mo increases, the crystallization temperatures will decrease.

Fig. 2 shows the change of DC permeability with annealing temperatures of $Fe_{73.5}Cu_1Nb_{3-x}Mo_xSi_{13}B_{9.5}$ (x= 0~ 3). It is seen that there are the optimum annealing temperature region for the $Fe_{73.5}Cu_1Nb_{3-x}Mo_xSi_{13}B_{9.5}$ (x= 0~ 3) alloys. Within this annealing temperature region, they have the highest

① [Received date] 2001- 05- 17; [Accepted date] 2001- 07- 17

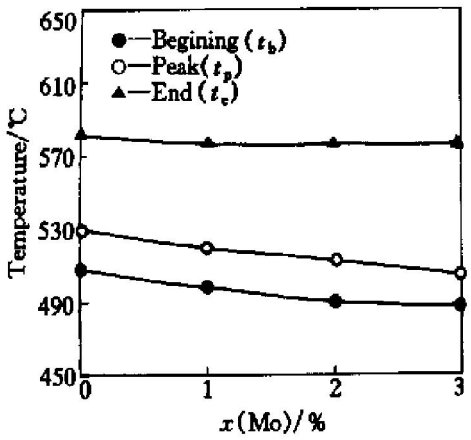

Fig. 1 Crystallization temperature with Mo content for $Fe_{73.5}Cu_1Nb_{3-x}Mo_xSi_{13}B_{9.5}$ (x = 0~ 3) alloys

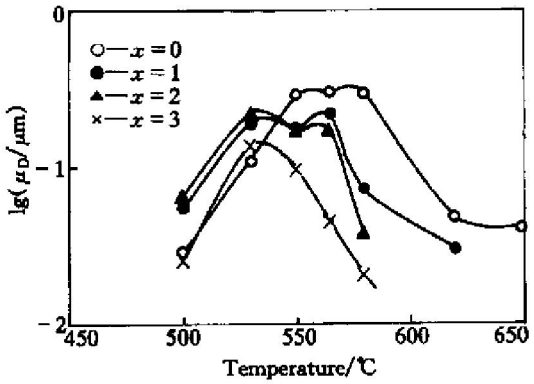

Fig. 2 DC permeability with annealing temperature of $Fe_{73.5}Cu_1Nb_{3-x}Mo_xSi_{13}B_{9.5}$ (x = 0~ 3) alloys

DC permeability. The optimum annealing temperature lowers with increasing Mo content. Meanwhile, except $Fe_{73.5}Cu_1Mo_3Si_{13}B_{9.5}$ alloy, others all have wider annealing temperature region.

Fig. 3 shows the change of AC permeability, which is under the condition of f = 1 kHz and H_m = 0.3 A/m, with annealing temperatures of $Fe_{73.5}Cu_1Nb_{3-x}Mo_xSi_{13}B_{9.5}$ (x = 0~ 3). It is seen that all

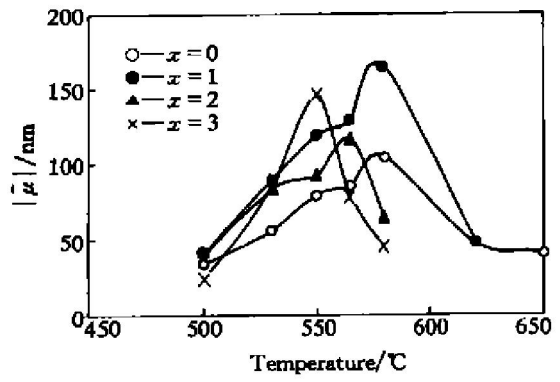

Fig. 3 AC permeability $|\tilde{\mu}|$ with annealing temperature of $Fe_{73.5}Cu_1Nb_{3-x}Mo_xSi_{13}B_{9.5}$ (x = 0~ 3) alloys

alloys have also the optimum annealing temperature for the AC permeability.

The microstructure of Finemet alloys consists of a lot of nano-crystallites and little boundary amorphous structure. Therefore, the annealing temperature should be selected between T_p to T_e. According to Fig. 2 and Fig. 3, the optimum annealing temperature can be obtained. Fig. 4 shows the optimum annealing temperature for DC and AC properties of $Fe_{73.5}Cu_1Nb_{3-x}Mo_xSi_{13}B_{9.5}$ (x = 0~ 3) alloys. The optimum annealing temperature for DC and AC decreases with increasing Mo content.

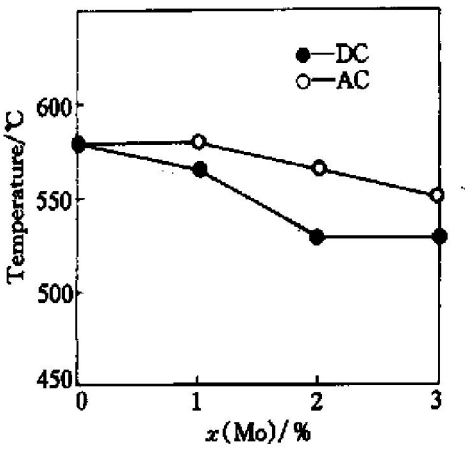

Fig. 4 Optimum annealing temperature as function of Mo content for $Fe_{73.5}Cu_1Nb_{3-x}Mo_xSi_{13}B_{9.5}$ (x = 0~ 3) Finemet alloys

3.2 Effect of content of Mo on permeability, saturation flux and coercivity

In Fig. 5, the change in the optimum DC permeability μ_m as function of Mo content and in the optimum AC relative permeability $\mu_{0.3/1k}$ (H_m = 0.3 A/m, f = 1 kHz) is reported. It is clear that the optimum DC permeability is reduced substantially by Mo substitution, while the optimum AC permeability varies up and down less dramatically. Alloy $Fe_{73.5}Cu_1Nb_3Si_{13}B_{9.5}$ shows the highest DC permeability. Contrary to the DC permeability, the alloys contained

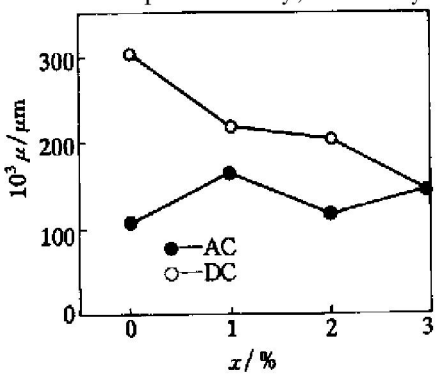

Fig. 5 Optimum DC and AC permeability as function of Mo content for $Fe_{73.5}Cu_1Nb_{3-x}Mo_xSi_{13}B_{9.5}$ (x = 0~ 3) Finemet alloys

Mo element have higher AC permeability $|\tilde{\mu}|$ than that of alloy without Mo content. The alloy $Fe_{73.5}Cu_1Nb_2Mo_1Si_{13}B_{9.5}$ shows the highest AC permeability.

From Fig. 1, we know that the ability of element Nb on restricting crystallite growth is stronger than element Mo. After annealing treatment, the size of crystallite of $Fe_{73.5}Cu_1Nb_3Si_{13}B_{9.5}$ alloy is smaller than other alloys contain element Mo. Even though the annealing temperature of $Fe_{73.5}Cu_1Nb_3Si_{13}B_{9.5}$ alloy is higher, it still exists the smallest grain size. Fig. 6 shows two TEM photos of alloys $Fe_{73.5}Cu_1Nb_3Si_{13}B_{9.5}$ and $Fe_{73.5}Cu_1Mo_3Si_{13}B_{9.5}$, the size of alloy $Fe_{73.5}Cu_1Nb_3Si_{13}B_{9.5}$ is much smaller than that of alloy $Fe_{73.5}Cu_1Mo_3Si_{13}B_{9.5}$. By measuring, the grain size of alloys, which were annealed in the optimum annealing temperature, is listed Table 1.

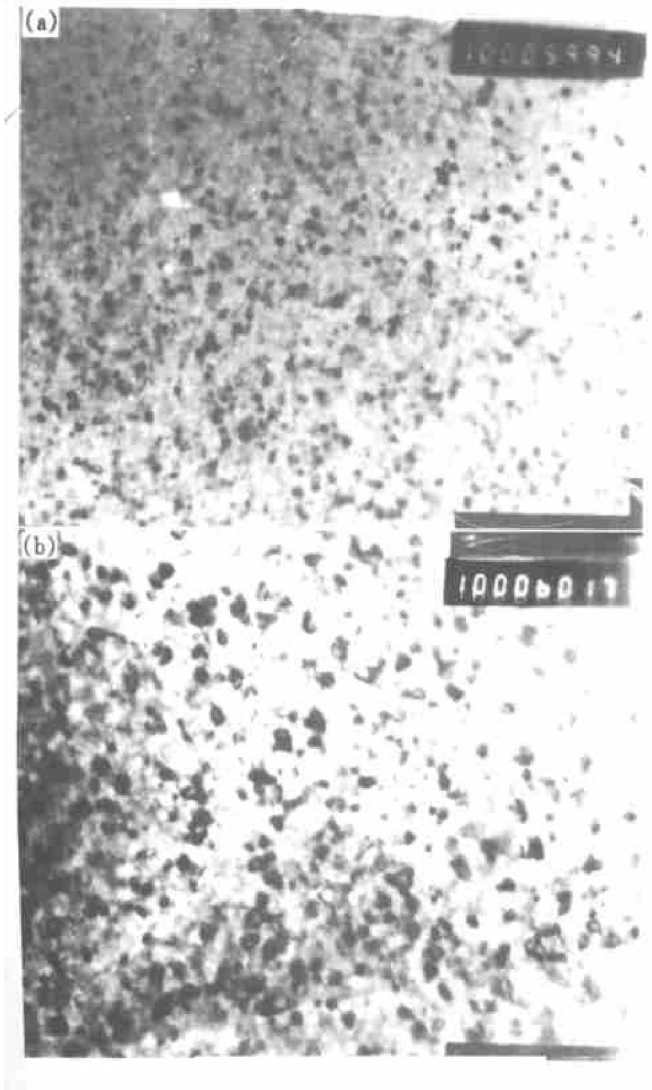

Fig. 6 TEM images of $Fe_{73.5}Cu_1Nb_3Si_{13}B_{9.5}$ alloy
(a) —Annealed at 580 ℃; (b) —Annealed at 530 ℃

According to the magnetization principle, the soft magnetic properties are depended on the saturation magnetization J_S, magnetostriction coefficient λ_S and anisotropy coefficient of grains K_1. The permeability is direct ratio to the saturation magnetization J_S and inverse ratio to the magnetostriction coefficient λ_S and anisotropy coefficient of grains K_1. After the $Fe_{73.5}Cu_1Nb_{3-x}Mo_xSi_{13}B_{9.5}$ alloy annealed, the amorphous structure is transformed into nano-crystalline structure. The ordered transformation of structure makes J_S increasing. Annealing treatment can also reduce magnetostriction coefficient λ_S and anisotropy coefficient of grains K_1. The formation of nano-crystalline makes λ_S decrease about as 10 times as amorphous alloys[11]. The saturation magnetization J_S increasing and the magnetostriction coefficient λ_S decreasing makes Finemet alloys have higher permeability.

Table 1 Grain size of different alloys after annealing (nm)

$x = 0$ (580 ℃)	$x = 1$ (565 ℃)	$x = 2$ (530 ℃)	$x = 3$ (530 ℃)
7.0~ 17.6	8.5~ 18.3	8.5~ 18.1	9.5~ 25.0

The size of grains is also an important factor to the soft magnetic properties, in the exchange interaction length L_{ex} (about 35~ 40 nm), primary permeability μ_i is reverse ratio to D^6 and the coercivity H_C is direct ratio to D^6 (D is grain size). The smaller grain size makes $Fe_{73.5}Cu_1Nb_3Si_{13}B_{9.5}$ alloy process higher DC permeability and smaller H_C. As adding Mo can increases specific resistance of amorphous alloy[8], it makes the samples contained Mo reveal higher AC permeability.

Fig. 7 shows the change in the saturation flux density B_S as a function of Mo content for the $Fe_{73.5}Cu_1Nb_{3-x}Mo_xSi_{13}B_{9.5}$ ($x = 0$~ 3) alloy. The larger B_S was obtained in the alloys added elements Nb and Mo together (B_S= 1.305 when x= 1%, B_S= 1.358 when x= 2%).

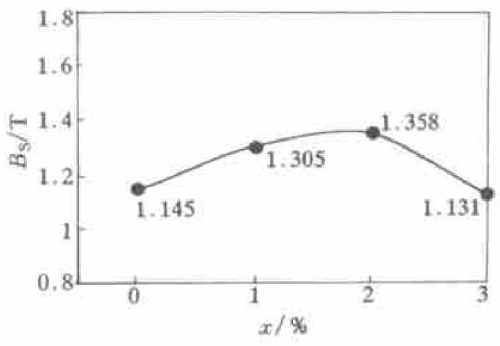

Fig. 7 Saturation flux density B_S as function of Mo content for $Fe_{73.5}Cu_1Nb_{3-x}Mo_xSi_{13}B_{9.5}$ ($x = 0$~ 3) Finemet alloys

Fig. 8 shows the effect of Mo content on the coercivity H_C. With increasing Mo content, the coercivity is increased. However, for x = 1% ~ 2% in

Mo substituted alloys, H_C is smaller than 3 A/m. Therefore, reasonably good soft magnetic properties are retained.

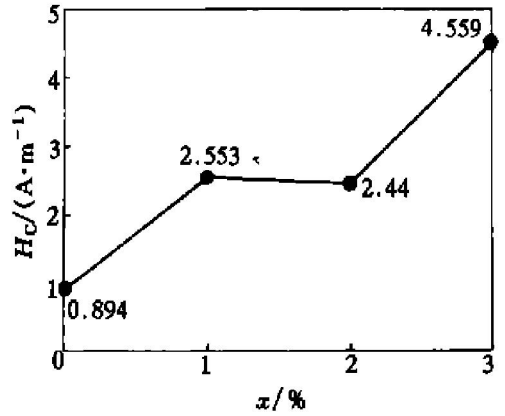

Fig. 8 Coercivity H_C as function of Mo content for $Fe_{73.5}Cu_1Nb_{3-x}Mo_xSi_{13}B_{9.5}$ (x = 0~ 3) Finemet alloys

3.3 Effect of Mo content on frequency dependence

In Fig. 9, the frequency dependence of the optimum AC relative permeability for $Fe_{73.5}Cu_1Nb_{3-x}Mo_xSi_{13}B_{9.5}$ (x = 0~ 3) Finemet alloys in the range of 50~ 10 kHz is shown. We can see that samples that contain Mo show higher AC permeability than that of alloy without Mo after non-magnetic field annealing. When x = 1%, the alloy exists the highest AC permeability in various frequency. AC permeability decreases with frequency. When the frequency is closed to 10 kHz, the permeability of all alloys is quite identical.

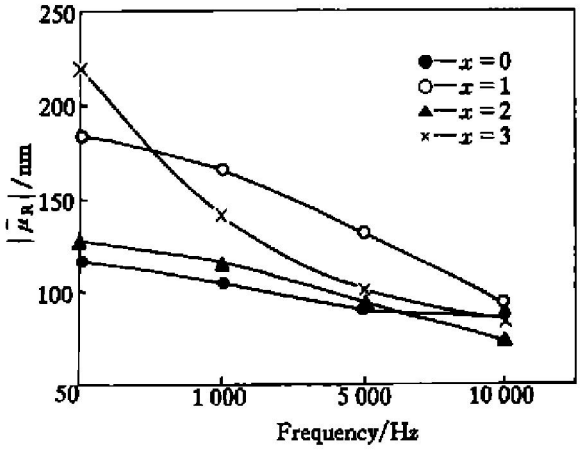

Fig. 9 Frequency dependence of AC relative permeability for $Fe_{73.5}Cu_1Nb_{3-x}Mo_xSi_{13}B_{9.5}$ (x = 0~ 3) Finement alloys

Fig. 10 shows the frequency dependence of core loss for $Fe_{73.5}Cu_1Nb_{3-x}Mo_xSi_{13}B_{9.5}$ (x = 0~ 3) Finemet alloys in range of 50~ 10 kHz at B_m = 0.2 T. It is seen that $Fe_{73.5}Cu_1Nb_2Mo1Si_{13}B_{9.5}$ alloy annealed at optimum temperature has the lowest core loss.

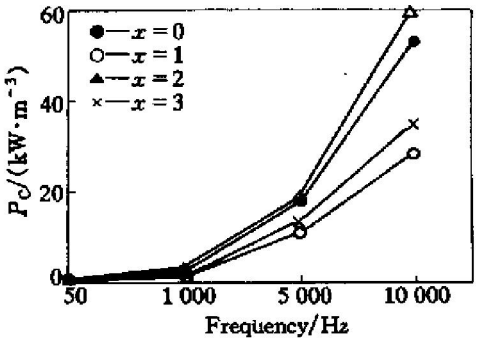

Fig. 10 Frequency dependence of core loss (P_C) for $Fe_{73.5}Cu_1Nb_{3-x}Mo_xSi_{13}B_{9.5}$ (x = 0~ 3) Finemet alloys

[REFRENCES]

[1] Yoshizawa Y, Oguma S, Yamauchi K. New Fe-based soft magnetic alloys composed of ultrafine grain structure [J]. Journal of Applied Physics, 1988, 64(10): 6044-6046.

[2] Yoshizawa Y, Yamauchi K. Magnetic properties of Fe-Cu-M-Si-B (M= Cr, V, Mo, Nb, Ta, W) alloys [J]. Materials Science and Engineering, 1991, A133: 176-179.

[3] Zhukova V, Cobeno A F, Pina E, et al. Study of the magnetic properties of $Fe_{73.4-x}Cu_1Nb_{3.1}Si_{13.4+x}B_{9.1}$ ($1.1 \leqslant x \leqslant 1.6$) microwires [J]. Materials Science and Engineering A, 2000, 215(6): 322-324.

[4] Raja M M, Chattopadhyay K, Majumdar B, et al. Structure and soft magnetic properties of Finemet alloys [J]. Journal of Alloys and Compounds, 2000, 297(1-2): 199-205.

[5] Ramin D, Riehemann W. Dependence of softmagnetic properties of nanocrystalline Finemet on surface defects [J]. Zeitschrift Fur Metallkunde, 1999, 90(11): 938-942.

[6] Varga R, Vojtanik P, Konc M. Low-field magnetic properties of amorphous and nanocystalline FeCrCuNbSiB alloys [J]. Journal of Magnetism and Magnetic Materials, 2000, 215: 340-342.

[7] Yoshizawa Y, Yamauchi K. Effects of magnetic field annealing on magnetic properties in ultrafine crystalline Fe-Cu-Nb-Si alloys [J]. IEEE Transaction on Magnetism, 1989, 25: 3324-3326.

[8] Herzor G. Grain structure and magnetism of nanocrystalline ferromagnets [J]. IEEE Transaction on Magnetism, 1989, 25: 3327-3329.

[9] Zhou X Z, Morrish A H. Mossbaur study of amorphous and nanocrystalline $Fe_{73.5}Cu_1Nb_3Si_{13.5}B_9$[J]. Journal of Applied Physics, 1993, 73(10): 6597-6599.

[10] Knobel M, Sato Turtelli R. Composition evolution and magnetic properties of nanocrystalline $Fe_{73.5}Cu_1Nb_3Si_{13.5}B_9$[J]. Journal of Applied Physics, 1992, 71(12): 6008-6012.

[11] Chen G J. New type soft magnetic materials—structure and magnetism of ultracrystalline alloy [J]. Research in Metallic Material, (in Chinese), 1991, 19(4): 17-27.

[12] Zhang Y Z. The magnetic properties and application of Fe-based ultracrystalline alloys [J]. Shanghai Steel Research, (in Chinese), 1992, 5: 1-10.

(Edited by HUANG Jin-song)